Intermediates and kinetics of membrane fusion

Joe Bentz
Department of Bioscience and Biotechnology, Drexel University, Philadelphia, Pennsylvania 19104

ABSTRACT Recently, it has become clear that the influenza virus fusion protein, hemagglutinin (HA), produces membrane destabilization and fusion by a multistep process, which involves the aggregation of the HAs to form a fusion site. While the details of this process are under debate, it is important to recognize that proposing any sequence of "microscopic" fusion intermediates encumbers general "macroscopic" kinetic consequences, i.e., with respect to membrane mixing rates. Using a kinetic scheme which incorporates the essential elements of several recently proposed models, some of these measurable properties have been elucidated. First, a rigorous mathematical relationship between fusion intermediates and the fusion event itself is defined. Second, it is shown that what is measured as the macroscopic "fusion rate constant" is a simple function of all of the rate constants governing the transitions between intermediates, whether or not one of the microscopic steps is rate limiting. Third, while this kinetic scheme predicts a delay (or lag) time for fusion, as has been observed, it will be very difficult to extract reliable microscopic information from these data. Furthermore, it is predicted that the delay time can depend upon HA surface density even when the HA aggregation step is very rapid compared with fusion, i.e., the delay time need not be due to HA aggregation. Fourth, the inactivation process observed for influenza virions at low pH can be described within this kinetic scheme simply, yet rigorously, via the loss of the fusion intermediates. Fifth, predicted Arrhenius plots of fusion rates can be linear for this multistep scheme, even though there is no single rate-determining step and even when a branched step is introduced, i.e., where one pathway predominates at low temperature and the other pathway predominates at high temperature. Furthermore, the apparent activation energies obtained from these plots bear little or no quantitative resemblance to the microscopic activation energies used to simulate the data. Overall, these results clearly show that the intermediates of protein mediated fusion can be studied only by using assays sensitive to the formation of each proposed intermediate.

INTRODUCTION

To know the molecular mechanism of viral envelope fusion implies knowing which viral protein causes fusion, whether other viral (or target) membrane proteins play a role in that fusion, what parts of the viral fusion protein are responsible for bilayer destabilization and what parts are responsible for completing the fusion event. In principle, a fusion site may involve multiple copies of several different proteins. The essential question is that of the architecture of the fusion site, i.e., the spatial and temporal arrangement of all of the proteins involved. The architecture is determined by which parts of each protein induce the bilayer destabilization and how this destabilization evolves.

Recently, several detailed models have been proposed to explain how the fusion protein of influenza virus, hemagglutinin (HA), actually produces membrane destabilization and fusion (Bentz et al., 1990, 1992; Bentz, 1991; Stegmann et al., 1990, 1991; Stegmann and Helenius, 1992; Blumenthal et al., 1991; Clague et al., 1992; Siegel, 1992). All of these models include the aggregation of HAs within the host membrane surface, together with various reconfigurations of the HAs leading to the fusion event with the target membrane. Regardless of which, if any, of these models is correct, it is essential to recognize that proposing any sequence of "fusion intermediates" creates a mass action kinetic model of fusion with certain measurable properties.

To address this issue, a kinetic scheme is developed which incorporates the essential features of all of the proposed models in the fewest number of steps. The objective is not to show how one may choose between the various models. Actually, the various models are kinetically very similar. Rather, the point is to illustrate the general kinetic behavior of all of the models which have been proposed. Only with these "generic" properties clearly in mind, can we proceed to construct the experiments which will illuminate the correct mechanism.

The results of this study are fivefold. First, a simple but rigorous relationship between fusion intermediates and the fusion event itself is defined. Second, it is shown that what is measured as the macroscopic "fusion rate constant" (see, Nir et al., 1992) is a reasonably simple function of all of the rate constants governing the transitions between the fusion intermediates. This implies that the macroscopic fusion rate constant depends upon all of the microscopic rate constants, even if one of the microscopic steps is rate limiting. This result is somewhat counterintuitive, but it is very important with respect to elucidating fusion mechanisms. Third, it has been noted that there can be a delay (or lag) time for fusion, which is especially prominent at low temperature (Morris et al., 1989; Stegmann et al., 1990; Clague et al., 1991, 1992; Stegmann and Helenius, 1992). Here, it is shown that while these delay times can be simulated by the proposed kinetic scheme, it is very difficult to extract reliable microscopic information from these data, e.g., the number of fusion proteins at the fusion site. In fact, the simulated delay times show a dependence upon HA surface density

0006-3495/92/08/448/12 $2.00

even when the delay time is not due to HA aggregation. Fourthly, it has been noted that influenza virions can inactivate at low pH, such that they lose the capacity to fuse over time (White et al., 1982; Sato et al., 1983). Nir and colleagues have incorporated this process into their kinetic analysis of fusion by appending a time dependence onto the macroscopic fusion rate constant (Stegmann et al., 1989; Nir et al., 1990, 1992). Here, the inactivation process is described directly via the loss over time of the fusion intermediates, which yields predictions for fusion kinetics in agreement with the previous studies.

Finally, the fifth result concerns the usefulness of Arrhenius plots. It is shown that the multistep kinetic scheme proposed here can simulate observed fusion kinetics very well, that the Arrhenius plots of these simulated fusion data can be quite linear and that the "apparent" activation energies, derived from these plots, bear little quantitative similarity to the "true" activation energies of the fusion intermediate transitions used for the simulation in the first place. Remarkably, even postulating a branched step within the overall fusion mechanism, wherein at low temperatures (0°C), one pathway predominates and at high temperatures (37°C), another pathway predominates, can yield linear Arrhenius plots for the macroscopic fusion kinetics. Thus, a linear Arrhenius plot is neither evidence for a single rate-limiting step nor even a single mechanistic route.

STEPS OF VIRUS-CELL AGGREGATION AND FUSION

Previous work has shown that the general sequence of binding and fusion reactions of small particles (viruses, liposomes or vesicles) with large particles (cells) is given by (Bentz et al., 1988),

$$V + AF_{i-1,j} \underset{D_{i-1,j}}{\overset{C_{i-1,j}}{\rightleftharpoons}} AF_{ij} \xrightarrow{f_{ij}} AF_{i-1,j+1}, \qquad (1)$$

where V is the small particle (i.e., virus, liposome or vesicle) which is binding to the cell. AF_{ij} denotes the cell with i-bound and j-fused vesicles. C_{ij} is the rate constant for aggregation of a vesicle to a cell with i-bound and j-fused cells, D_{ij} is the dissociation rate constant and f_{ij} is the fusion rate constant. If the cell has N_B binding sites which are identical and independent, then

$$C_{ij} = \frac{N_B - i - j}{N_B} C$$
$$D_{ij} = (i + 1)D$$
$$f_{ij} = if, \qquad (2)$$

where $C = C_{00}$, $D = D_{00}$ and $f = f_{10}$, i.e., the rate constants when there are no other competing bound or fused liposomes. These equations are based on assumptions which are certainly correct when only a few vesicles/virions have bound and fused per cell. Thus, the system of viruses fusing with cells can be used to measure the macroscopic fusion rate constant, f, of a single virion. The next question is what does this rate constant mean with respect to fusion intermediates.

Stages of membrane fusion

After close apposition of the membranes, fusion is comprised of several distinct stages:

(a) lateral reorganization of membrane fusion proteins to form aggregates;

(b) destabilization of the outer monolayers of the membranes by the formation of intermembrane intermediates, denoted II, formed by protein and/or lipid bridges within the protein aggregate;

(c) formation of the fusion pore, denoted FP, which is defined as the initial communication of the internal aqueous compartments. If the pore is lipid lined, then mixing of the inner monolayers of the membranes will occur. This step can be monitored by initial conductance between the HA expressing cell and the target vesicle, while breakage of the pore would be monitored by conductance and capacitance flickering (Spruce et al., 1989, 1991);

(d) formation of the fusion site, denoted FS, which is defined as a stable joining of the two membranes. This step would be monitored by complete lipid and contents mixing (Sarkar et al., 1989) or the establishment of infinite conductance between the HA expressing cell and the target vesicle (Spruce et al., 1989, 1991) or the release of the nucleocapsid into the cellular cytoplasm.

These are the common elementary steps of the current models which have been proposed to explain HA-mediated fusion (Bentz et al., 1990, 1992; Bentz, 1991; Stegmann et al., 1990, 1991; Stegmann and Helenius, 1992; Blumenthal et al., 1991; Clague et al., 1991, 1992; Siegel, 1992). An essential first step of exposure of the NH_2-terminus of HA2 is not included because it is rapid compared with the fusion reaction (Stegmann et al., 1990), although in at least one strain it may not become fully exposed at low temperature (Brunner et al., 1991).

In addition, Stegmann et al. (1990) have proposed that before step (a), the fusion peptide of HA inserts into the target membrane. While it is generally agreed that this fusion peptide is required for the fusion reaction, just how it performs its task is debatable. Insertion was studied only at low temperature, 0°C, using influenza virus strains which either fused with liposomes only very slowly compared with the peptide insertion kinetics (Stegmann et al., 1991) or did not fuse at all with the liposomes (Brunner and Tsurudome, 1992). Whether insertion occurs before or after HA aggregation is unknown. Whether insertion represents an essential step in fusion, or is merely one pathway accessible to HAs(while the fusion event is mediated by HA2 NH_2-termini which have not inserted) has not yet been resolved (Bentz et al.,

1992; Stegmann and Helenius, 1992; Siegel, 1992; Brunner and Tsurudome, 1992). As we will discover below, the resolution of these questions will not be easy.

Regardless of these contentions, and despite the possibility that there may be other steps involved, the mass action kinetics of the four steps listed above can simulate any of the data thus far obtained for HA mediated fusion. Having peptide insertion occur before step *a*, above, would make the analysis more complex, without altering any of the basic conclusions.

KINETIC MODEL OF FUSION INTERMEDIATES

Fusion protein aggregation

Step *a* is the aggregation of HAs on the surface. On virions, this step is likely to be rapid, in that the glycoproteins may already be arranged, due either to their high surface density or interactions with other membrane or matrix proteins. On HA expressing cells, this aggregation appears to be an unfavorable event, which may be highly reversible (Ellens et al., 1990; Bentz et al., 1990). On infected cells, it is only known that HA clustering is a natural part of the budding of the virus. Regardless, this step can be modeled as a mass action process with different initial conditions, which for our purposes lead to the same basic conclusions.

The minimal fusion unit is defined as the minimal aggregate size of HAs which can sustain fusion. This number is denoted ω, i.e., an aggregate of ω HAs or more is required to create a fusion site. The initial rate of fusion will depend on the number of aggregates of size ω (i.e., ω-lets). As the total surface density of HA increases, the number of ω-lets and higher order aggregates at a given time increases. Comparing the change in the number of fused liposomes to the change in the HA surface density can fix the value of ω (Bentz, 1991).

To begin, let $[X_0]$ denote the total HA trimer surface density and $[X_i(t)]$ denote the surface density of the i-mer aggregates of HA at time t, i.e., $[X_1(t)]$ is the surface density of singlets and $[X_3(t)]$ is the surface density of triplets, i.e., an aggregate of 3 HA trimers. Conservation of mass implies that $[X_0] = \sum_{j=1}^{\infty} j[X_j(t)]$, at all times.

The concentrations of these various species will depend on the association constant between the HAs, which are,

$$X_1 + X_1 \underset{r_{11}}{\overset{a_{11}}{\rightleftharpoons}} X_2 \qquad (3)$$

$$X_1 + X_2 \underset{r_{12}}{\overset{a_{12}}{\rightleftharpoons}} X_3,$$

and so on with higher order reactions. Aggregation could cease at some particular size or fusion could occur only with some optimal aggregate size, i.e., ω would then be that optimal size. For simplicity, it will be assumed that if a triplet (X_3) can induce fusion; then so can higher order aggregates. This is a weak assumption in that for the cases of most physical interest, the concentration of the aggregates larger than the minimal fusion unit is insignificant, relative to the ω-lets, so that fusion would be mediated mostly by the ω-lets in any case. Thus, the surface density of fusion competent aggregates is,

$$S_\omega(t, [X_0]) = \sum_{j=\omega}^{\infty} [X_j(t)], \qquad (4)$$

$S_\omega(t, [X_0])$ has been evaluated as a function of $[X_0]$ for a variety of special cases (Bentz and Nir, 1981*a*, *b*; Bentz, 1991).

Fusion intermediates

The other steps of fusion proceed from the HA aggregate. Step (*b*) is the formation of the intermembrane intermediate (denoted II) from those HA ω-lets which are "aimed" at the target membrane. Let δ denote the area of HA-containing membrane which is closely apposed to target membrane. Then, $\sigma_\omega(t) = \delta S_\omega(t, [X_0])$ is the number of aggregates which are capable of forming intermembrane intermediates. If $S_\omega(t, [X_0])$ is not uniform over the cell surface, then $\sigma_\omega(t)$ could be defined for each patch. Note that δ, and thus $\sigma_\omega(t)$, are proportional to the total number of bound virions or vesicles, which is denoted N_v below.

Step (*c*) is the transformation of the intermembrane intermediate to the fusion pore (denoted FP), which can either break back to an HA aggregate (which would result in the conductance/capacitance flickering observed by Spruce et al., 1989, 1991) or progress to a fusion site (denoted FS), through which large molecular weight aqueous space markers (e.g., nucleocapsids) can flow. The kinetic pathway for these steps is,

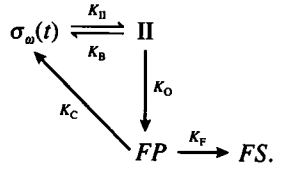

(5)

In general, it could be argued that the step from II to FP might be reversible, e.g., the fusion pore closes to the intermembrane intermediate, rather than back to the HA aggregate. Including such a step significantly complicates the mathematical equations which describe this kinetic pathway, without altering any of the conclusions which we shall reach. This can be shown simply, but rigorously, using a Laplace transform analysis. For simplicity, then, the potential reversibility of $FP \rightarrow$ II will be ignored. Thus, formal solutions to these kinetic equations can be written as,

$$[II] = K_{II} G_\omega(K_1, t)$$

$$[FP] = \frac{K_{II} K_O}{K_1 - K_2} (G_\omega(K_2, t) - G_\omega(K_1, t))$$

$$[FS] = \frac{K_{II} K_O K_F}{K_1 K_2} \times \left(\int_0^t \sigma_\omega(s)\, ds + \frac{K_2 G_\omega(K_1, t) - K_1 G_\omega(K_2, t)}{(K_1 - K_2)} \right), \quad (6)$$

where,

$$G_\omega(K, t) = \exp\{-Kt\} \int_0^t \exp\{Ks\} \sigma_\omega(s)\, ds$$

$$K_1 = K_O + K_B$$

$$K_2 = K_C + K_F.$$

MACROSCOPIC FUSION FROM MICROSCOPIC INTERMEDIATES

We are now in a position to relate the microscopic rates of fusion intermediate formation to the macroscopic rates of membrane fusion observed via fluorescence assays. The exact construction of this analysis will depend upon whether the chosen assay monitors fusion pores, fusion sites or both. Sarker et al. (1989) noted that the initial kinetics of lipid mixing from erythrocyte ghosts labeled with the fluorophor octadecylrhodamine, which partitions only into the exterior monolayer, or of contents mixing from erythrocytes loaded with the soluble fluorophor NBD-taurine were similar during fusion of erythrocyte ghosts with HA-expressing fibroblasts. This would imply that both assays were responding to the formation of the fusion site. Other assays will monitor the formation of both the fusion site and the fusion pore, e.g., conductivity (Spruce et al., 1989, 1991) or lipid labels which are on both inner and outer monolayers (Stegmann et al., 1989, 1990). For simplicity, this analysis will follow the kinetics of formation of the fusion site, which is the final step of the process. The analysis of the formation of the fusion pore is similar.

The key to connecting the microscopic and macroscopic equations is the number of fusion sites per bound vesicle or virion, which is given by

$$\eta(t) = [FS]/N_v \quad (7)$$

where N_v is the number of vesicles (liposomes, erythrocytes, et cetera) or virions bound per bell. The same type of prescription would hold in the case of virions fusing with labeled liposomes (Stegmann et al., 1989, 1990). To calculate the fraction of bound vesicles or virions which have fused, it is assumed that each fusion site is independent. Any other assumption, e.g., that fusion occurs via some aggregate of fusion pores, is currently unnecessary. Then, because the total number of cells and virions/vesicles used in an experiment is large, the probability that a given bound vesicle or virion is connected to the cell by j fusion sites is given by a Poisson distribution, i.e.,

$$p_j = \frac{\eta(t)^j}{j!} \exp\{-\eta(t)\}. \quad (8)$$

Therefore the fraction of bound vesicles which have fused, $F(t)$, is just the probability that any vesicle is connected by one or more fusion sites, i.e.,

$$F(t) = \sum_{j=1}^{\infty} p_j = 1 - \exp\{-\eta(t)\}. \quad (9)$$

This is our first result, i.e., a simple but rigorous relationship between the fusion intermediates and the observed fusion kinetics. With a fusion assay which measures both fusion pores and fusion sites, the measured fusion is obtained by defining $\eta(t)$ relative to the sum of the surface densities of these two species.

To further analyze the fusion kinetics, it is necessary to specify the protein aggregation kinetics. As described in Bentz (1991), this can be a complicated problem, but a great deal can be learned by examining two extreme cases. The first case is when the fusion reaction is very slow compared with the protein aggregation kinetics and, so, protein aggregation is effectively at equilibrium. The second case is when the protein aggregation kinetics are rate limiting to the fusion reaction.

With the HA expressing cells, Ellens et al. (1990) showed that the lateral diffusion coefficient of the HAs was consistent with free diffusion through the lipid bilayer. Thus, the collision frequency between HAs is very high. We also found that the number of HAs involved in fusion intermediates is small compared with the total number expressed on the cell surface. With over 10^6 HAs expressed per cell and over 1,200 glycophorin liposomes bound per cell (via approximately 5 HA-glycophorin contacts each), less than 1.5% of the bound liposomes fused within 90 s. No matter how rough these estimates may be, it is reasonable to assume that much less than 1% of the HAs were involved in binding or fusion. This would also imply that HA aggregation on these cells is very reversible and very rapid compared with fusion, as has been suggested by others (Stegmann et al., 1990; Clague et al., 1991). This also implies that the loss of an HA aggregate due to fusion has no significant effect upon the HA aggregation kinetics, because such a small fraction of the total amount HA is consumed by fusion.

Thus, a plausible assumption to make for the HA expressing cells is that the HA aggregation is at equilibrium on the cell surface. For virions, if the fusion proteins are held in place, then this assumption of equilibrium would still be appropriate. This assumption will permit simple closed form expressions for the macroscopic fusion rate constant to be developed, which will clearly show the basic relationship between the microscopic and macroscopic events. For generality, the case where the HA ag-

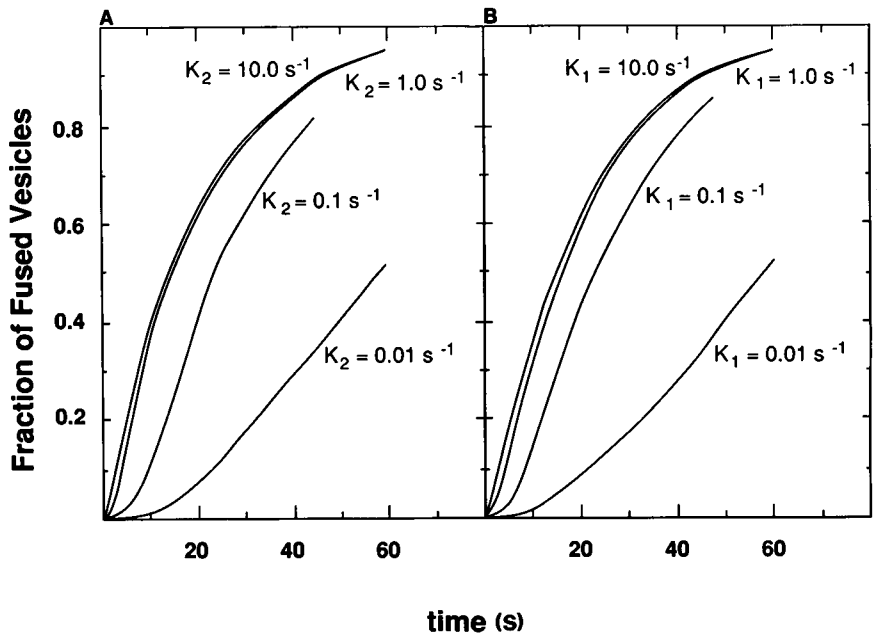

FIGURE 1 Fusion [$F(t)$] as a function of time is calculated from Eqs. 9 and 11. In A, $K_1 = 2.0\ s^{-1}$ and several values of K_2 are considered. In B, $K_2 = 1.0\ s^{-1}$ and several values of K_1 are considered. $C\overline{\sigma_\omega} = 0.05\ s^{-1}$ in all cases.

gregation is rate limiting to fusion will be considered in an Appendix, where it is found that in the proper time domain, the same basic conclusions obtained here also hold.

Thus, when HA aggregation is rapid with respect to fusion, $\sigma_\omega(t)$ can be approximated by its equilibrium distribution value, i.e.,

$$\sigma_\omega(t) \rightarrow \overline{\sigma_\omega} = \overline{\sigma_\omega}([X_0]), \tag{10}$$

where the bar indicates the equilibrium value. Evaluation of $\overline{\sigma_\omega}$, relative to $[X_0]$, follows directly from the reactions described in Eq. 3, as described in Bentz and Nir (1981*a*, *b*). Here it is only important to note that it is constant in time, which implies that

$$G_\omega(K, t) = \frac{\overline{\sigma_\omega}}{K}(1 - \exp\{-Kt\})$$
$$\eta(t) = C\overline{\sigma_\omega}\left(t - \frac{K_1^2(1 - \exp\{-K_2 t\}) - K_2^2(1 - \exp\{-K_1 t\})}{K_1 K_2 (K_1 - K_2)}\right), \tag{11}$$

where,

$$C = \frac{K_{II} K_O K_F}{K_1 K_2 N_v}.$$

Recall that since $\overline{\sigma_\omega}$ is proportional to N_v, the product $C\overline{\sigma_\omega}$ is independent of N_v.

Macroscopic fusion rate constant

This gives us our second result, because it is quite obvious that even when the rate constant for the formation of the fusion site is absolutely rate limiting, i.e., $K_F \rightarrow 0$, $K_2 t \gg 1$ and $K_1 t \gg 1$, the measured fusion will be

$$F(t) = 1 - \exp\{-C\overline{\sigma_\omega} t\}, \tag{12}$$

which depends upon all of the microscopic rate constants, as well as the HA surface density.

Nir and colleagues have modeled the aggregation and fusion kinetics between several viruses and several cell lines using Eqs. 1 and 2, without explicit account of these postulated fusion intermediates, and they were able to obtain adequate fits (see reviews in Nir et al., 1990, 1992). To the extent that the assumption of equilibrium in HA aggregation is correct, the fusion rate constant they measured $f = C\overline{\sigma_\omega}$ in these cases.

A more quantitative estimate for which the kinetics of formation of the fusion intermediates can be ignored is shown in Fig. 1. The fusion curves, $F(t)$, are shown for a variety of values of K_1 and K_2. In A, where $K_1 = 2.0\ s^{-1}$, we see that the kinetics of intermediate formation are irrelevant to the fusion kinetics whenever $K_2 > 1.0\ s^{-1}$. In B, where $K_2 = 1.0\ s^{-1}$, we see that the kinetics of intermediate formation are irrelevant to the fusion kinetics whenever $K_2 > 1.0\ s^{-1}$. Here $C\overline{\sigma_\omega} = 0.05\ s^{-1}$, but changing the value of $C\overline{\sigma_\omega}$ merely changes the overall time scale of the fusion process without a major effect on the shape of the curves. Thus, the cases fitted by Nir and colleagues were systems where both K_1 and K_2 were large compared with $f = C\overline{\sigma_\omega}$, as might be expected.

In fact, Eq. 12 has very important implications with respect to our ability to elucidate multistep, first-order processes like membrane fusion. In particular, it is not true that the macroscopic, or overall, rate constant equals the rate constant of the rate limiting step or that only those factors which affect the slowest step of the process can be observed. Suppose that the rate constant

K_F drastically changes (for whatever reason) at some temperature. An example of this would be the lipid bilayers becoming competent to undergo a phase transition at some temperature (see, Alford et al., 1991). Then, Eq. 12 implies that the overall, observed rate of fusion will respond to that phase transition under all but one condition. If, and only if, $K_F \gg K_C$ and $K_F \gg K_O + K_B$, does $\eta(t)$, and therefore the fusion via Eq. (9), become independent of K_F. This is equivalent to claiming that the intermembrane intermediate, II, proceeds directly to the fusion site, FS, with a rate constant of K_O, see Eq. 5. Because these reactions are first order, a significant change in any of the rate constants will be observed in the macroscopic fusion rate constant, unless that step is infinitely faster than all of the other steps, which is equivalent to saying that this step can never be seen.

NUMBER OF FUSION SITES AND THE MINIMAL FUSION UNIT

It is also clear how the data presented Ellens et al. (1990) on the number of bound liposomes which fused with the HA expressing cells could be used to count the number of fusion sites per liposome and estimate the minimal fusion unit. There the fraction of bound liposomes which fuse within 90 s were counted for two cell lines which expressed different HA surface densities. These fractions were very small, <1.5%, which from Eq. 9 implies that $F(t) \approx \eta(t)$, i.e., the average number of fused liposomes equals the average number of fusion sites. Therefore, for all practical purposes, these data were measuring initial rates of fusion site formation.

For the sake of generality, let λ denote the ratio of HA surface densities, which was 1.9 in Ellens et al. (1990), then

$$\frac{F(t, \lambda[X_0])}{F(t, [X_0])} \approx \frac{\eta(t, \lambda[X_0])}{\eta(t, [X_0])} = \frac{\overline{\sigma_\omega}(\lambda[X_0])}{\overline{\sigma_\omega}([X_0])} = \frac{\overline{S_\omega}(\lambda[X_0])}{\overline{S_\omega}([X_0])}, \quad (13)$$

where it has been assumed that the areas of contact per bound liposome and that the number of bound liposomes per cell are independent of the HA surface density, which is reasonable because the liposomes and their binding constants to the cells were found to be the same for both cell lines. Therefore, the ratio of fusion extents at 90 s is equal to the ratio of the surface densities of fusion competent HA aggregates. Furthermore, as shown in Bentz (1991),

$$\frac{\overline{S_\omega}(\lambda[X_0])}{\overline{S_\omega}([X_0])} \to \lambda^\omega \quad \text{when} \quad (a_{11}/r_{11})[X_0] \to 0 \quad (14)$$

Thus, in the limit of small values of the product of the HA surface density times the association constant for aggregation, the ratio of the fusion efficiencies equals the ratio of HA surface densities raised to the power of the minimal fusion unit.

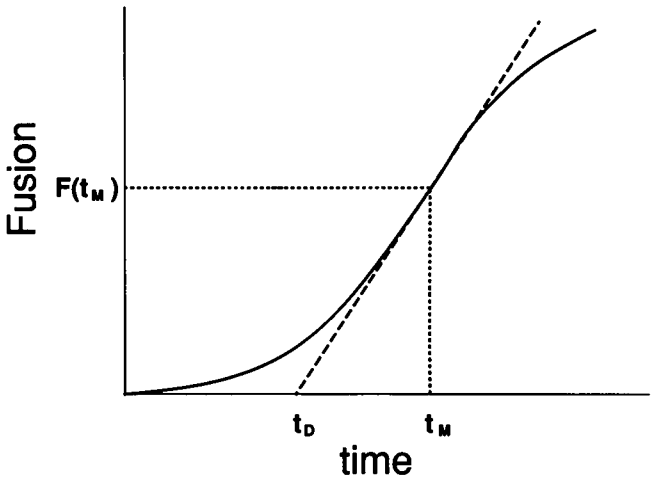

FIGURE 2 Typical graph of fusion vs time when there is a delay or lag time for fusion. The fusion intensity curve, $F(t)$, is the solid line. t_M denotes the time at which the fusion rate is maximal. The delay time, t_D, is defined by the x-intercept of the dashed line, which is the tangent to the curve at the time where the fusion rate is maximal. Mathematically, the fusion rate, $F'(t_M)$, is maximal at time t_M and the second derivative of the fusion curve at this time, $F''(t_M) = 0$, because this is an inflection point of the graph.

At this time, it is not known whether for the cell lines used that the HA surface density was small enough to use Eq. 14, because the HA-association constant (a_{11}/r_{11}) is unknown. Thus, Ellens et al. (1990) could only conclude that $\omega \geq 2$. On the other hand, it may be noted that in the simplest possible case, where $a_{11} \approx 4$ (lateral surface diffusion coefficient of HA) $\approx 10^{-9}$ (HA/cm^2)$^{-1}$ s^{-1} (Torney and McConnell, 1983; Ellens et al., 1990), $r_{11} \leq$ (lipid lateral jump frequency) $\approx 10^8$ s^{-1} (Galla et al., 1979; Vaz et al., 1984) and all of the HAs on the surface are accessible for fusion (i.e., $[X_0] \approx 10^{11}$ HA/cm^2; Ellens et al., 1990), then $(a_{11}/r_{11})[X_0] \geq 10^{-6}$. While this calculation is very rough and neglects activation energies, it is interesting that this lower bound is four orders of magnitude smaller than the value required for Eq. 14 to be substantially correct (Bentz, 1991, 1992). Thus, Eq. 14 may not be entirely off the mark.

DELAY TIMES FOR FUSION

Several studies have noted that the fusion of influenza virus or HA expressing cells does not start immediately after the pH is lowered, but rather, there is a delay or lag (Stegmann et al., 1989, 1990; Morris et al. 1989; Sarkar et al., 1989; Clague et al., 1991). It has been claimed that this delay time is dependent upon HA surface density (Clague et al., 1991). If true, does this imply that the delay time is due to the HA aggregation step and can one extract the minimal fusion unit from measurements of the delay times as reliably as can be done using the ap-

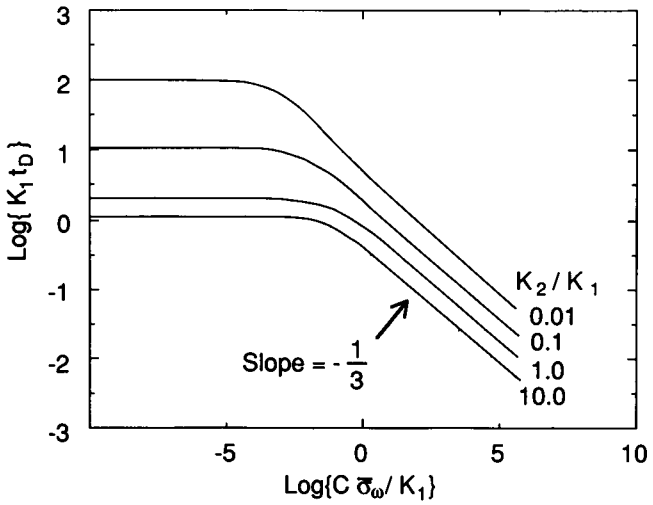

FIGURE 3 Graph of the delay time as a function of surface density of fusion competent HA aggregates, from Eq. 18. Actually, $\log\{K_1 t_D\}$ is plotted as a function of $\log\{C\overline{\sigma_\omega}/K_1\}$, for several values of K_2/K_1. When the surface density is small, i.e., $C\overline{\sigma_\omega} \to 0$, then the delay time is independent of the HA surface density, in that $K_1 t_D \to 1 + K_1/K_2$. Thus, in this regime, the delay time cannot predict the minimal fusion unit. When the surface density is large, which is when t_M and t_D become small, then $\log\{K_1 t_D\} \to \log\{(4K_1/K_2)^{1/3}(3 - e^{2/3})/2\} - \frac{1}{3}\log\{C\overline{\sigma_\omega}/K_1\}$.

proach described in the previous section. The answer to both these questions is no.

To discuss delay times, we need a consistent definition and one which is used in practice (Stegmann et al., 1990, 1991). Under the conditions where delay times are observed, the graph of fusion vs time is sigmoidal. The delay time can be defined from the tangent to the curve at the time where the fusion rate is maximal, as shown in Fig. 2. The fusion intensity curve, $F(t)$, is the solid line and the tangent line at the maximal rate is the dashed line. t_M denotes the time at which the fusion rate is maximal and delay time, t_D, is defined by the x-intercept of the dashed line. Mathematically, the fusion rate, $F'(t_M)$, is maximal at time t_M and the second derivative of the fusion curve at this time, $F''(t_M) = 0$, because this is an inflection point of the graph. One can see how the curves shown in Fig. 1 would predict delay times in the range of 2–20 s. Clague et al. (1991) defined the delay time according to when the fluorescence rises above background. While this definition has certain advantages, it is mathematically imprecise, it depends upon calibration standards and it is more arbitrary in execution.

We want to relate the delay time to the number of fusion sites per bound liposome using Eq. 9. Because the time of the maximal fusion rate, t_M, is defined by $F''(t_M) = 0$, differentiating Eq. 9 twice with respect to time implies that t_M is equivalently defined as the time when,

$$(\eta'(t_M))^2 = \eta''(t_M) \tag{15}$$

and the delay time of fusion, t_D, defined by $F'(t_M) = F(t_M)/(t_M - t_D)$, is equal to

$$t_D = t_M - [\exp\{\eta(t_M)\} - 1]/\eta'(t_M). \tag{16}$$

Now we can use these equations to derive explicit estimates for the dependence of t_D on the fusion protein surface density. When protein aggregation is at equilibrium, which is very likely to be the case with the HA expressing cells and perhaps with the virions, Eq. 15 can be solved using Eq. 11 to show that t_M is fixed as the solution to,

$$C\overline{\sigma_\omega} = \frac{K_1K_2(K_1 - K_2)(\exp\{-K_2t_M\} - \exp\{-K_1t_M\})}{(K_1(1 - \exp\{-K_2t_M\}) - K_2(1 - \exp\{-K_1t_M\}))^2}. \tag{17}$$

The dimensionless form of this equation is

$$\frac{C\overline{\sigma_\omega}}{K_1} = \frac{\kappa(1 - \kappa)(\exp\{-\kappa\mu\} - \exp\{-\mu\})}{((1 - \exp\{-\kappa\mu\}) - \kappa(1 - \exp\{-\mu\}))^2}, \tag{18}$$

where $\kappa = K_2/K_1$ and $\mu = K_1t_M$.

Fig. 3 shows the graph of $\log\{K_1t_D\}$ vs $\log\{C\overline{\sigma_\omega}/K_1\}$, for several values of K_2/K_1. When the HA surface density is small, i.e., $C\overline{\sigma_\omega}/K_1 \to 0$, then the delay time is independent of the HA surface density, in that $K_1t_D \to 1 + K_1/K_2$. Thus, in this regime, the delay time cannot predict the minimal fusion unit.

When the surface density is relatively large, which is when t_M and t_D become small, then $\log\{K_1t_D\} \to \log\{(4K_1/K_2)^{1/3}(3 - e^{2/3})/2\} - \frac{1}{3}\log\{C\overline{\sigma_\omega}/K_1\}$. Therefore, in this domain, the delay time will show a dependence upon the HA surface density and the minimal fusion unit. If it were the case that $\overline{\sigma_\omega}$ was proportional to $[X_0]^\omega$, as described in Eq. 14, then the slope of the graph log {delay time} vs log {HA surface density} would be equal to $\omega/3$. Unfortunately, $\overline{\sigma_\omega}$ only becomes a simple function of the HA surface density when the surface density becomes small, i.e., in the opposite limit.

It is worth emphasizing here that the predicted dependence of the delay time on HA surface density is not due to HA aggregation kinetics, since it was assumed that the HA aggregates are at equilibrium. Simply put, the smaller HA surface densities yield fewer HA aggregates and so the time required for the formation of the first fusion site increases. In the Appendix, the case where HA aggregation is rate limiting to fusion (and, hence, the delay) is analyzed. It is shown that while the delay time would depend upon HA surface density raised to the power $\omega/(\omega + 2)$, this case may not be realistic.

Thus, in general, the slope of the graph log {delay time} vs log {HA surface density} cannot be assumed to predict the minimal fusion unit ω in any simple way. All that can be said is that three times the value of this slope will be an underestimate of the minimal fusion unit. Reports of slopes of less than one third (Blumenthal et al., 1991; Clague et al., 1991) are consistent with this conclusion, although the implication would be that the minimal fusion unit was less than one, which led these au-

thors to suggest that the delay time did not offer a means to measure the minimal fusion unit. On the other hand, these same studies relied upon important assumptions, e.g., that infected cells had uniform HA surface densities and that partially trypsinized HA0, the inactive precursor of HA, could be expressed as fractions of fusogenic HA trimers. These assumptions must be verified before further speculation is warranted. In any event, it is clear that the delay time is not as simple a function of the HA surface density as is the number of fused liposomes.

VIRAL INACTIVATION

Nir and colleagues analyzed the process of influenza virus inactivation, wherein the virions at low pH lose the capacity to fuse with target membranes over time. They fitted this process via a time dependent decrease in the value of the macroscopic fusion rate constant f (Stegmann et al., 1989; Nir et al., 1990, 1992). Microscopically, inactivation can be treated at the level of the HAs, either in Eq. 3 if it is due to conformational changes in the isolated protein or protein aggregates or in Eq. 5 if it occurs at the stage of the fusion units. It is important to note that this inactivation has not been observed with HA expressing cells (Ellens et al., 1990), even though the virions from the same HA strain show roughly 50% inactivation (Puri et al., 1990). This may reflect a difference between the characteristics of HA on virions and on cells.

Under conditions of inactivation, it is clear that $\sigma_\omega(t)$ is time dependent. While it is not yet known how HA is inactivated, for the sake of illustration, let it be assumed that it occurs from the aggregated HA. Then the fusion intermediate reaction scheme would look like,

$$\begin{array}{ccccc} \sigma_\omega(t) & \underset{K_B}{\overset{K_{II}}{\rightleftharpoons}} & \mathrm{II} & & \\ \downarrow{\scriptstyle K_I} & \nwarrow{\scriptstyle K_C} & \downarrow{\scriptstyle K_O} & & \\ IHA & & FP & \xrightarrow{K_F} & FS, \end{array} \tag{17}$$

where *IHA* denotes inactivated HA. For the sake of simplicity, we further assume that on the virus the HA aggregates are preformed and reversibility can be ignored. That is $K_C = K_B = 0$, which implies that $\sigma_\omega(t) = \sigma_\omega(0) \times \exp\{-K_t t\}$, where $\sigma_\omega(0)$ is the initial surface density of fusogenic aggregates and $K_t = K_{II} + K_I$. Less restrictive assumptions could be made at the price of significantly more complex equations, but the basic conclusions would remain exactly the same. For this case,

$$\eta(t) = C\sigma_\omega(0)\left(\frac{1-\exp\{-K_t t\}}{K_t} - \frac{K_1(\exp\{-K_t t\} - \exp\{-K_2 t\})}{(K_2 - K_t)(K_t - K_2)} + \frac{K_2(\exp\{-K_t t\} - \exp\{-K_1 t\})}{(K_1 - K_t)(K_1 - K_2)}\right). \tag{20}$$

The most interesting point here, even with these overly simple assumptions, is that some rather sophisticated

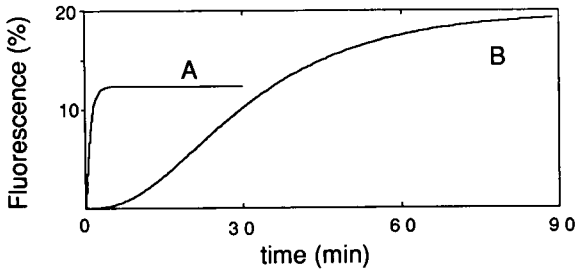

FIGURE 4 Calculated fluorescence curves which simulate the data of Stegmann et al. (1990) for the fusion of influenza virus with ganglioside liposomes at 37°C (*A*) and 0°C (*B*). These fits are not unique and therefore cannot be used to predict the real microscopic rate constants. However, these fits do demonstrate that the model shown in Eq. 15 does contain all of the kinetic complexity currently required to describe the data, using reasonable activation energies to develop a temperature dependence. Stegmann et al. (1990) measured fusion using octadecylrhodamine labeled virions and mixed equal mol ratios of viral and liposome phospholipids, which ideally would have produced about 50% of maximal fluorescence dequenching if each virion fused with one liposome. This was not tested, but for the sake of consistency in this simulation, let it be assumed that %fluorescence = $50(1 - \exp\{\eta(t)\})$. Other parameters used were: $C\sigma_\omega(0) = 0.02\ s^{-1}$, $K_1 = 0.02\ s^{-1}$, $K_2 = 0.05\ s^{-1}$ and $K_t = 0.07\ s^{-1}$ for *A* (the "37°C" data) and $C\sigma_\omega(0) = 0.0006\ s^{-1}$, $K_1 = 0.001\ s^{-1}$, $K_2 = 0.025\ s^{-1}$ and $K_t = 0.0012\ s^{-1}$ for *B* (the "0°C" data). The temperature dependencies amount to activation energies of only 14–18 kcal/mol, see Fig. 5 for more details. This simulation is not unique, in that other sets of constants produce similar curves.

data can be simulated quite well. Fig. 4 shows calculated fusion curves using Eqs. 9 and 20, which simulate the data of Stegmann et al. (1990) for influenza virus fusing with ganglioside liposomes at 37°C (*A*) and 0°C (*B*).

The simulations are quite good. Stegmann et al. (1990) suggest that the difference in extents of fluorescence dequenching with temperature is that at 37°C the virions are undergoing inactivation. However, if the fluorescence calibration is even roughly correct, then the simulation would imply that there is HA inactivation even at 0°C (*B*), because the curve does not reach 50%. For the model shown in Eq. 19, the extents of fluorescence are reached when $\eta(\infty) = C\sigma_\omega(0)/K_t$. The possibility that inactivation occurs at all temperatures has also been raised by Nir et al. (1992).

Eq. 20 is not identical to the equivalent equations used in Nir et al. (1991, 1992), see also Stegmann et al. (1989), to simulate inactivation. This is not important, because they have tested two very different time dependencies for the "macroscopic fusion rate constant" and did not find any significant difference with respect to "fitting the data." Eq. (20) can also yield good fits to these data. The real issue is whether the model "parameters" being fitted can be experimentally verified by some other type of experiment and theoretically defined with respect to molecular calculations. The microscopic formulation described here is certainly more compatible with molecular calculations.

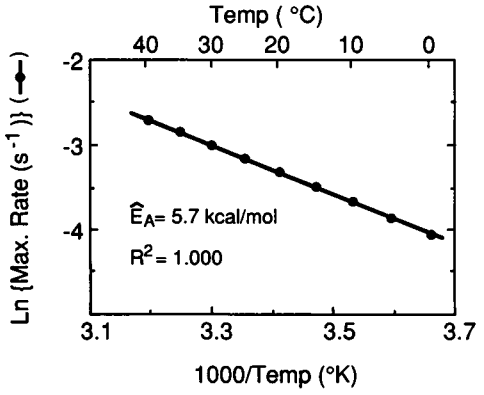

FIGURE 5 Arrhenius plot of the maximal rate of fluorescence intensity change for the data described in Fig. 4, shown by the data dots (●) and the least-squares fitted straight line. The absyssa is 1,000 divided by the temperature in degrees Kelvin. The top scale shows the temperature in degrees Celsius. Briefly, the maximal fusion rate, $F(t_M)$, was obtained from Eqs. 9, 15, and 20. All rate constants were assumed to have "Arrhenius" temperature dependencies, i.e., $K_x(T) = K_x(\infty) \times \exp\{-E_{ax}/RT\}$, where RT is the gas constant time the temperature in degrees Kelvin and x denotes any reaction step. While K_1 and K_2 represent the sum of two elementary rate constants (see Eq. 6), each with their own Arrhenius forms, for simplicity we will assume a single activation energy. As will become evident in the following, rigorously considering two more activation energies would not have any effect on the basic conclusions. The activation energies for the microscopic rate constants fixed by the rate constant values chosen at 0°C and 37°C for the simulation in Fig. 4 and were: E_{a1} = 14 kcal/mol for K_1, E_{a2} = 14 kcal/mol for K_2, E_{ai} = 18 kcal/mol for K_i, and $E_{aC\sigma}$ = 16 kcal/mol for $C\sigma(0)$. It is not necessary to consider the temperature dependencies of C and $\sigma(0)$ separately. The apparent activation energy of the fusion data, i.e., the slope of the fitted line times 1.98, is $\hat{E}_A$ = 5.7 kcal/mol, while the correlation coefficient is R^2 = 1,000. Obviously, the apparent activation energy obtained from the maximal rate of fusion bears little quantitative similarity to the underlying activation energies.

ARRHENIUS PLOTS AND MULTIPLE PATHWAYS TO FUSION

Stegmann et al. (1990) studied the temperature dependence of fusion of influenza virus with ganglioside containing liposomes, to investigate the possibility of whether the fusion reaction could be better studied at low temperature where everything happens more slowly. When they graphed the temperature dependence of the maximal fusion rates as an Arrhenius plot, measured by lipid mixing and defined as in Fig. 2, a nominally straight line was obtained. The fusion kinetics between influenza virus and erythrocyte ghosts also yielded a nominally straight line for its Arrhenius plot, albeit with a much different slope than that found for the ganglioside containing liposomes. From this linearity, Stegmann et al. (1990, 1991) suggested that the same mechanism of fusion was followed at low and high temperatures.

This is an important claim, because our ability to dissect the fusion reaction at low temperature is considerably greater, due to the slowness of all the reactions. However, because fusion is a multistep process, the meaning of an Arrhenius plot is unclear. We have already seen that the "macroscopic" fusion rate constant is a mixture of all of the underlying microscopic rate constants. So it is likely that the observed activation energy will depend upon the activation energies of all the underlying rate constants.

Fig. 5 shows this to be the case, which is the Arrhenius plot of the maximal fusion rates defined by the simulation in Fig. 4. While all of the microscopic rate constants are chosen to have activation energies of ~15 kcal/mol (see legend to Fig. 5 for the exact values), the apparent activation energy is $\hat{E}_A$ = 5.7 kcal/mol. Variations of ±1 kcal/mol in each of the underlying activation energies led to changes in $\hat{E}_A$ of roughly ±0.2 kcal/mol in the case of K_1, ±0.02 kcal/mol in the case of K_2, ±0.2 kcal/mol in the case of K_i and ±0.4 kcal/mol in the case of $C\sigma(0)$. Certainly, these sensitivities depend upon the values chosen for the rate constants and their activation energies. Nevertheless, the apparent activation energy is not due to some simple ratio of the microscopic rate constants, despite the fact that the least-squares fit is perfectly linear.

This proves that a linear Arrhenius plot does not imply that a single step of a multistep process is being observed. A more important question is whether a linear Arrhenius plot implies that the same mechanism is being observed, i.e., could fusion intermediates form by two different pathways?

Consider the following extension to the original fusion intermediate system, at the step of intermembrane intermediate conversion to fusion pore,

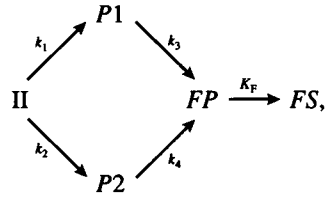

(21)

where $P1$ and $P2$ denote states in the alternative pathways. The question is whether the fusion pores, FP, can be formed via pathway 2 at high temperatures, 37°C, and via pathway 1 at low temperatures, 0°C, such that the Arrhenius plot of the maximal fusion rate, as defined in Figure 5, will be linear. Some arbitrary choices will need to be made to illustrate the answer, but it is a clear yes. Whether the branch begins at the intermembrane intermediates or the HA aggregates or earlier makes no difference for the conclusions we reach.

For simplicity, and to keep the number of adjustable parameters to a minimum, assume that all other steps of the overall fusion mechanism, either prior to and after the branched step shown in Eq. 21, are set to be very rapid, so that changes in the fusion rate with temperature will reflect just the kinetics of the branched step. This will give the clearest view of how such a branched pathway within the fusion process can affect the data. The

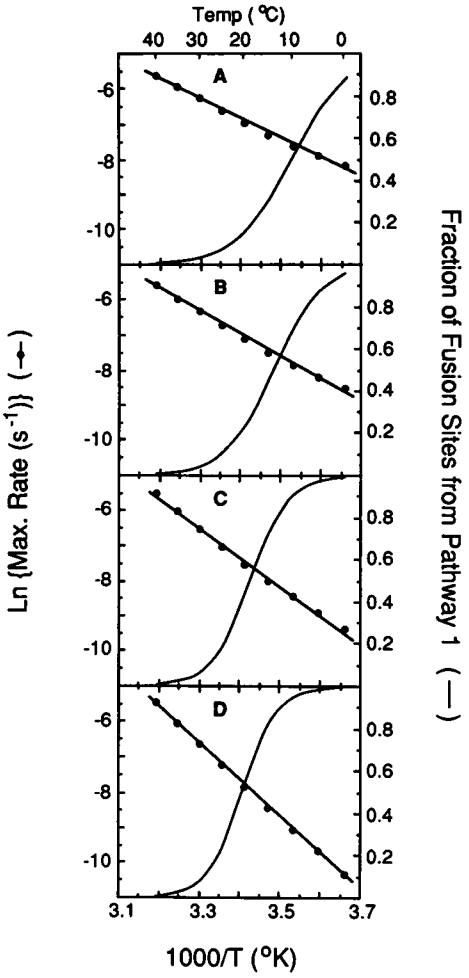

FIGURE 6 Arrhenius plots of the maximal rate of fluorescence intensity change when the branched pathway shown in Eq. 21 occurs, shown by the data dots (●) and the fitted straight line. All of the other rate constants (in Eqs. 5 or 19) were set to be infinitely fast, so that the fusion kinetics depended only upon the branched pathway. The right-hand ordinate is the fraction of the total number of fusion pores which arise via pathway 1 up to time of the maximal rate, t_M, which is shown by the sigmoidal smooth line. In all cases, $k_1(37°C) = k_3(37°C) = 0.001\ s^{-1}$ and $k_2(37°C) = k_4(37°C) = 0.01\ s^{-1}$. Setting $k_2(37°C)/k_1(37°C) = 10$ and $k_3(37°C)/k_4(37°C) = 10$ was done so that pathway 2 would be strongly predominant at 37°C. As shown, less that 1% of the fusion sites form from pathway 1 at 37°C, where $1/T(°K) = 3.66 \times 10^{-3}$. Setting $k_1(37°C) = k_3(37°C)$ and $k_2(37°C) = k_4(37°C)$ was arbitrary, but other reasonable choices, consistent with strongly favoring pathway 1 at 37°C, would not affect the basic properties of these graphs. Choosing $k_2(37°C) = 0.01\ s^{-1}$ was done so that the half-time of fusion at this temperature was ~1 min. It is assumed that the rate constants of the branched pathway have an "Arrhenius" form, i.e., $k_x(T) = k_x(\infty)\exp\{-E_{bx}/RT\}$, where RT is the gas constant time the temperature in degrees Kelvin and x denotes any reaction step. In all cases shown in the figure, $E_{b1} = 5$ kcal/mol. A has $E_{b2} = 20$ kcal/mol, B has $E_{b2} = 30$ kcal/mol, C has $E_{b2} = 40$ kcal/mol, and D has $E_{b2} = 50$ kcal/mol, to show the wide range of values for which linear plots can be obtained. The values of the other parameters is given in Table 1. The values of E_{b3} and E_{b4} were chosen, within 5 kcal/mol or so, to maximize both the linearity of the Arrhenius plot and the low temperature predominance of pathway 1. In all cases, these maxima were very broad, in that many different values of E_{b3} and E_{b4} would give quite similar results to those shown in the panels. Roughly, in order that over 90% of the fusion sites form from pathway 1 at 0°C, $E_{b2} + E_{b4}$ must exceed $E_{b1} + E_{b3}$ by at least 30 kcal/mol. The Arrhenius plot becomes more linear as the values of E_{b2}, E_{b3} and E_{b4} become more equal. Choosing E_{b1} to be some other value, say 20 kcal/mol, would not change the fact that the Arrhenius plots can be brought to linearity by appropriate changes in the values of E_{b2}, E_{b3} and E_{b4}, as described in Table 1.

TABLE 1 **Parameters of the Arrhenius Plots shown in Fig. 6**

Panel	E_{b1} [a]	E_{b2}	E_{b3}	E_{b4}	$\hat{E}_A$ [b]	R^2 [b]
		kcal/mol			*kcal/mol*	
A	5	20	20	35	11.0	0.995
B	5	30	25	35	12.5	0.995
C	5	40	35	40	16.1	0.999
D	5	50	45	50	20.5	0.999
[c]	15	35	30	45	15.3	0.994
[c]	15	45	40	50	18.7	0.997
[c]	25	45	40	55	19.7	0.997

[a]These are the activation energies for the rate constants shown in Eq. (21), i.e. for the branched pathway. [b]$\hat{E}_A$ is 1.98 times the least squares fitted slope of the graph of $\log_e$ {Max. Rate} vs. $1/T$ (°K), i.e. it is the apparent activation energy of the maximal fusion rate. R^2 is the correlation coefficient for the least squares fit. [c]These cases are not shown in the figure, but satisfy the criteria of nearly linear plots ($R^2 > 0.99$) and greater than 95% of the fusion sites being formed from pathway 2 at 40°C.

solutions to these kinetic reactions are straightforward to obtain, but will not be shown here.

Fig. 6 shows the Arrhenius plots for the maximal fusion rates for a wide range of activation energies for the rate constant k_2, together with the least-squares fitted slopes. Clearly, the linear fits are excellent. Also shown is the fraction of the total number of fusion pores which arise via pathway 1 up to time t_M, which ranges from less than 1% at 37°C to 99.9% at 0°C.

Table 1 shows the values of all of the parameters used in the calculations shown in Fig. 6. The values of the activation energies for k_3 and k_4 were chosen to give linear fits for the apparent activation energies and greater than 90% formation of the fusion sites via pathway 1 at 0°C, however, many values satisfied these criteria.

If the other reactions of the general fusion mechanism are not infinitely fast, then the presence of the branched step becomes even harder to discern by an Arrhenius plot, i.e., the plots are linear over even wider ranges of values for the branched step activation energies. These relatively complex first-order systems tend to smooth out Arrhenius plots, as indicated by Fig. 5.

Other values of the activation energies could be chosen which would yield highly nonlinear Arrhenius plots. Nevertheless, the important point is that linear Arrhenius plots can be obtained even when the mechanism completely shifts between two pathways over temperature. So, while a linear Arrhenius plot might be consistent with a single-step fusion mechanism, it is also consistent with a multistep branched fusion mechanism, and is therefore largely useless as a tool for defining these

mechanisms. Thus, the data showing that the fusion peptide of influenza virus inserts into target membranes before lipid mixing occurs at low temperature (Stegmann et al., 1991; Brunner and Tsurudome, 1992) cannot be extrapolated to infer that the same mechanism occurs at physiological temperatures solely based upon the linearity of Arrhenius plots. Direct measurements are required, presumably using rapid mixing techniques with photoaffinity labelling of HA. Fortunately, these same data should permit us to discover whether the insertion of the N-terminus of HA2 into the target membrane belongs to the same kinetic pathway as membrane fusion.

APPENDIX

Here, the case of protein aggregation rate limited fusion will be examined. In this case, $\sigma_\omega(t)$ must be explicitly evaluated in Eq. 6. However, with the HA expressing cells, it appears that few aggregates form, relative to the total number of HAs. This restricts the time domain over which protein aggregation can be rate limiting to fusion. It can be shown that only so long as $\tau = 2a_{11}[X_0]t \ll 1$, will the amounts of HAs in aggregates be small (Bentz and Nir, 1981*b*). At longer times, only aggregation reversibility and the establishment of the equilibrium distribution of aggregates can maintain this condition, which is the case described in the text. In the short time domain, Bentz and Nir (1981*b*) showed that the Smoluchowski solutions for aggregation reactions give adequate approximations. These solutions presume that the aggregation is irreversible, although that condition can be relaxed somewhat. Thus, when it is assumed that the fraction of HAs consumed by fusion is small (as described in the text), the aggregation reactions described by Eq. 3 imply that the concentration of j-mer protein aggregates is approximated by

$$\frac{[X_j(t)]}{[X_0]} \approx \frac{\tau^{j-1}}{(1+\tau)^{j+1}} \approx \tau^{j-1} \qquad (A.1)$$

where

$$\tau = 2a_{11}[X_0]t \ll 1$$

Then concentration of aggregates of size ω or larger at time t is,

$$S_\omega(t, [X_0]) \approx [X_0]\tau^{\omega-1} \qquad (A.2)$$

Thus,

$$G_\omega(K, t) = \frac{\delta(2a_{11}[X_0]t)^\omega}{2a_{11}\omega} \sum_{j=0}^{\infty} (-1)^j \frac{\omega!}{(\omega+j)!}(Kt)^j \qquad (A.3)$$

$$\eta(t) = C_1[X_0]^\omega t^{\omega+2} \times \left(1 - \frac{(K_1+K_2)t}{\omega+3} + \frac{(K_1^2+K_1K_2+K_2^2)t^2}{(\omega+3)(\omega+4)} + \cdots\right) \qquad (A.4)$$

where,

$$C_1 = \frac{\delta K_{II} K_O K_F (2a_{11})^{\omega-1}}{\omega(\omega+1)(\omega+2)N_v} \qquad (A.5)$$

For our purposes, it is adequate to approximate $\eta(t)$ by,

$$\eta(t) \approx C_1[X_0]^\omega t^{\omega+2} \exp\left\{-\frac{(K_1+K_2)t}{\omega+3}\right\}. \qquad (A.6)$$

Because $\eta(t)$ is small, $F(t) \approx \eta(t)$. It is now clear that the conclusions reached under conditions of equilibrium for HA aggregation also hold when the aggregation is slow compared with the fusion steps. Firstly, the macroscopic fusion rate constant is essentially $f \approx C_1[X_0]^\omega$, which will depend on each and every forward microscopic rate constant, even though here the HA aggregation step is rate limiting. Secondly, the ratio of the extents of fusion at given time will be equal to the ratio of HA surface densities raised to the power of the minimal fusion unit. Thirdly, while the delay time can be easily calculated from Eq. A.6 and the graph of the log {delay time} vs log $\{[X_0]\}$ will have a slope of $-\omega/(\omega+2)$, this simple relationship between the slope and the minimal fusion unit holds only for a very limited time regime. If HA aggregation were rate limiting to fusion and if the true delay time can be predicted from Eq. (A.6), then one could fix the minimal fusion unit from such a graph. Ironically, proving that these equations are appropriate would require that the macroscopic fusion rate constant depended upon the HA surface density as $[X_0]^\omega$, which would provide the minimal fusion unit directly. However, as was argued in the text, it is less likely that HA aggregation is rate limiting to fusion for the HAs expressed on cells or even those on virions, not to mention the fact that a $t^{\omega+2}$ time dependence for fusion has never been reported.

I wish to thank Drs. David Siegel and Shlomo Nir, and Dennis Alford for critically reading the manuscript.

Supported by National Institutes of Health grant GM-31506.

Received for publication 26 August 1991 and in final form 31 January 1991.

REFERENCES

Alford, D., H. Ellens, and J. Bentz. 1991. Fusion of influenza virus with glycophorin bearing liposomes: role of the target membrane. *Biophys. J.* 50:134*a*. (Abstr.)

Bentz, J. 1991. Membrane Fusion: Viral Fusion Proteins and Lipid Intermediates. *In* Advances in Membrane Fluidity. Vol. 5. R. C. Aloia, C. C. Curtain, and L. M. Gordon, editors. Alan R. Liss, Inc. New York. 259–287.

Bentz, J. 1992. Membrane fusion intermediate and the kinetics of membrane fusion. *In* Viral Fusion Mechanisms. J. Bentz, editor. CRC Press, Boca Raton, FL. In press.

Bentz, J., and S. Nir. 1981*a*. Aggregation of colloidal particles modeled as a dynamical process. *Proc. Natl. Acad. Sci. USA.* 78:1634–1637.

Bentz, J., and S. Nir. 1981*b*. Mass action kinetics and equilibria of reversible aggregation. *J. Chem. Soc. Faraday Trans.* I. 77:1249–1275.

Bentz, J., S. Nir, and D. Covell. 1988. Mass action kinetics of virus-cell aggregation and fusion. *Biophys. J.* 54:449–462.

Bentz, J., H. Ellens, and D. Alford. 1990. An architecture for the fusion site of influenza hemagglutinin. *FEBS (Fed. Eur. Biochem. Soc.) Lett.* 276:1–5.

Bentz, J., H. Ellens, and D. Alford. 1992. Architecture and mechanism of influenza hemagglutinin induced fusion. *In* Viral Fusion Mechanisms. J. Bentz, editor. CRC Press, Boca Raton, FL. In press.

Blumenthal, R., A. Puri, C. Schoch, and M. J. Clague. 1991. A dissection of steps leading to viral envelope protein-mediated membrane fusion. Ann. New York Acad. Sci. 635:285–296.

Brunner, J., and M. U. Tsurudome. 1992. Fusion-protein membrane interactions as studied by hydrophobic photo labelling. *In* Viral Fusion Mechanisms. J. Bentz, editor. CRC Press, Boca Raton, FL. In press.

Brunner, J., C. Zugliani, and R. Mischler. 1991. Fusion activity of influenza virus PR8/34 correlates with a temperature-induced con-

formational change within the hemagglutinin ectodomain detected by photochemical labelling. *Biochemistry.* 30:2432–2438.

Clague, M. J., C. Schoch, and R. Blumenthal. 1991. Delay time for influenza virus hemagglutinin-induced membrane fusion depends upon hemagglutinin surface density. *J. Virol.* 65:2404–2407.

Clague, M. J., C. Schoch, and R. Blumenthal. 1992. Towards a dissection of the influenza haemagglutinin mediated membrane fusion pathway. In Viral Fusion Mechanisms. J. Bentz, editor. CRC Press, Boca Raton, FL. In press.

Ellens, H., J. Bentz, D. Mason, F. Zhang, and J. White. 1990. Fusion of influenza hemagglutinin-expressing fibroblasts with glycophorin bearing liposomes: role of hemagglutinin surface density. *Biochemistry.* 29:9697–9707.

Galla, H. J., W. Hartmann, U. Thielen, and E. Sackmann. 1979. On two dimensional passive random walks in lipid bilayers and fluid pathways in biomembranes. *J. Membr. Biol.* 48:215–236.

Morris, S. J., D. P. Sarkar, J. M. White, and R. Blumenthal. 1989. Kinetics of pH-dependent fusion between 3T3 fibroblasts expressing influenza hemagglutinin and red cells. *J. Biol. Chem.* 264:3972–3978.

Nir, S., N. Düzgünes, M. Pedroso de Lima, and D. Hoekstra. 1990. Fusion of enveloped viruses with cells and liposomes: activity and inactivation. *Cell Biophys.* 17:181–201.

Nir, S., M. Pedroso de Lima, C. E. Larsen, J. Wilschut, D. Hoekstra, and N. Düzgünes. 1992. Kinetics and extent of virus-cell aggregation and fusion. *In* Viral Fusion Mechanisms. J. Bentz, editor, CRC Press, Boca Raton, FL. In press.

Puri, A., F. Booy, R. W. Doms, J. M. White, and R. Blumenthal. 1990. Conformational changes and fusion activity of influenza virus hemagglutinin of the H2 and H3 subtypes: effects of acid pretreatment. *J. Virol.* 64:3824–3932.

Sarkar, D. P., S. J. Morris, O. Eidelman, J. Zimmerberg, and R. Blumenthal. 1989. Initial stages of influenza hemagglutinin-induced cell fusion monitored simultaneously by two fluorescent events: cytoplasmic continuity and membrane mixing. *J. Cell biol.* 109:113–122.

Sato, B. S., K. Kawasaki, and S. Ohnishi. 1983. Hemolytic activity of influenza virus hemagglutinin glycoproteins activated by mildly acidic environments. *Proc. Natl. Acad. Sci. USA.* 80:3153–3157.

Siegel, D. 1992. Modeling protein-induced fusion intermediates: insights from the relative stability of lipidic intermediates. *In* Viral Fusion Mechanisms. J. Bentz, editor. CRC Press, Boca Raton, FL. In press.

Spruce, A. E., A. Iwata, J. M. White, and W. Almers. 1989. Patch clamp studies of single cell-fusion events mediated by a viral fusion protein. *Nature (Lond.).* 342:555–558.

Spruce, A. E., A. Iwata, and W. Almers. 1991. The first milliseconds of the pore formed by a fusogenic viral envelope protein during membrane fusion. *Proc. Natl. Acad. Sci. USA.* 88:3623–3627.

Stegmann, T., and A. Helenius. 1992. Intermediates in influenza induced membrane fusion. From models to mechanisms. *In* Viral Fusion Mechanisms. J. Bentz, editor. CRC Press, Boca Raton, FL. In press.

Stegmann, T., S. Nir, and J. Wilschut. 1989. Membrane fusion activity of influenza virus: effects of gangliosides and negatively charged phospholipids in target liposomes. *Biochemistry.* 28:1698–1704.

Stegmann, T., J. White, and A. Helenius. 1990. Intermediates in influenza induced membrane fusion. *EMBO (Eur. Mol. Biol. Org.) J.* 13:4231–4241.

Stegmann, T., J. M. Delfino, F. M. Richards, and A. Helenius. 1991. The HA2 subunit of influenza hemagglutinin inserts into the target membrane prior to fusion. *J. Biol. Chem.* 266:18404–18410.

Torney, D. C., and H. M. McConnell. 1983. Diffusion-limited reaction rate theory for two-dimensional systems. *Proc. R. Soc. Lond.* A387:147–170.

Tsurudome, M., R. Glück, R. Graf, R. Falchetto, U. Schaller, J. Brunner. 1992. Lipid interactions of the hemagglutinin HA2 N-terminal segment during influenza virus-induced membrabne fusion. *J. Biol. Chem.* In press.

Vaz, W. L. C., F. Goodsaid-Zaldunondo, and K. Jacobson. 1984. Lateral diffusion of lipids and proteins in bilayer membranes. *FEBS (Fed. Eur. Biochem. Soc.) Lett.* 174:199–207.

White, J. M. J. Kartenbeck, and A. Helenius. 1982. *EMBO (Eur. Mol. Biol. Org.) J.* 1:217–222.